

# Towards Language-guided Visual Recognition via Dynamic Convolutions

Gen Luo<sup>1</sup>, Yiyi Zhou<sup>1\*</sup>, Xiaoshuai Sun<sup>1</sup>, Xinghao Ding<sup>2</sup>, Yongjian Wu<sup>3</sup>,  
Feiyue Huang<sup>3</sup>, Yue Gao<sup>4</sup>, Rongrong Ji<sup>1</sup>

<sup>1</sup>Media Analytics and Computing Lab, Department of Artificial Intelligence,  
School of Informatics, Xiamen University, 361005, China.

<sup>2</sup>School of Informatics, Xiamen University, China. <sup>3</sup>YouTu Lab, Tencent.

<sup>4</sup>Software School of Tsinghua University.

luogen@stu.xmu.edu.cn, {zhouyiyi, xssun, dxh}@xmu.edu.cn,  
{littlekenwu, garyhuang}@tencent.com, gaoyue@tsinghua.edu.cn, rrji@xmu.edu.cn

## Abstract

In this paper, we are committed to establishing an unified and end-to-end multi-modal network via exploring the language-guided visual recognition. To approach this target, we first propose a novel multi-modal convolution module called *Language-dependent Convolution* (LaConv). Its convolution kernels are dynamically generated based on natural language information, which can help extract differentiated visual features for different multi-modal examples. Based on the LaConv module, we further build the first fully language-driven convolution network, termed as *LaConvNet*, which can unify the visual recognition and multi-modal reasoning in one forward structure. To validate LaConv and LaConvNet, we conduct extensive experiments on four benchmark datasets of two vision-and-language tasks, *i.e.*, visual question answering (VQA) and referring expression comprehension (REC). The experimental results not only shows the performance gains of LaConv compared to the existing multi-modal modules, but also witness the merits of LaConvNet as an unified network, including compact network, high generalization ability and excellent performance, *e.g.*, +4.7% on RefCOCO+.

## 1 Introduction

In recent years, the rapid developments of the joint vision-language study have been supported by a flurry of benchmark datasets [24, 2, 7, 15, 11, 17, 27, 14, 34] and methods [1, 13, 12]. The latest research trends [34, 13, 38, 28, 26] have gone beyond a simple understanding of multi-modal information [30, 48, 36], and focused on more advanced cognitive tasks, such as visual reasoning [49, 15, 24, 14], visual question answering [2, 7, 15, 14, 21], and referring expression comprehension [35, 24, 11, 17, 27].

To accomplish these tasks, most existing vision-and-language (VL) systems adopt a modular structure. As shown in Fig. 1 (a), a typical VL system often uses a visual backbone, *e.g.*, ResNet [9] or FasterRCNN [37], to extract the features of the input image, based on which another inference module is deployed to model the cross-modal interactions. This long-popular design paradigm has achieved great success in various VL tasks [2, 7, 15, 11], but has been also criticized for its excessive parameters and high computational overhead [19].

In contrast to this modular structure, we are committed to establishing an unified alternative by exploring language-guided visual recognition. As shown in Fig. 1-b, we aim at embedding the

\*Corresponding Author.

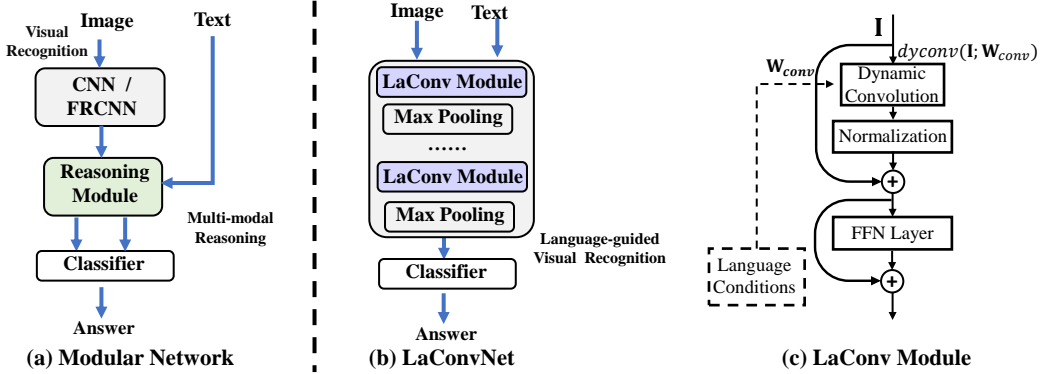


Figure 1: Comparison between the conventional modular network (a-b), and the illustration of the proposed LaConv module (c). LaConv can unify the visual recognition and multi-modal interaction into one processing step. Based on it, we further build an unified and end-to-end network called LaConvNet.

language information into the process of visual recognition, and then directly output the language-dependent visual features. This motivation is inspired by the human cognitive mechanism towards multi-modal tasks. Neuroscience researches [41, 29, 39, 4] show that the processing mechanism of *primary visual cortex cells* can be affected by other modalities, *e.g.*, text or sound, and then produce the multimodal sensory. It means that the low-level visual recognition can also be driven by the natural language signals. For example, after receiving a natural language instruction, people will perform the visual recognition related to the instruction, *e.g.*, paying attention to relevant regions and analyzing relevant information like colors or textures.

To achieve this target, we first propose a novel *Language-Guided Dynamic Convolution* (LaConv), of which structure is depicted in Fig. 1. The property of “*language-guided visual recognition*” are mainly reflected in that LaConv can realize differentiated feature extractions on the same image according to different natural language instructions. This property is attributed to its dynamic convolution filters predicted by natural language information. Through this novel multi-modal convolution, LaConv can complete visual recognition and multi-modal reasoning in one processing step.

In addition to a plug-in module for existing VL systems, we also exploit LaConv as a stand-alone block for building an unified multi-modal network. Specifically, we build the first fully language-guided convolution network with LaConv blocks, termed *LaConvNet*. As shown in Fig.1, LaConvNet processes the input image from the pixel level, and embeds the natural language information into the complete process of visual feature learning. The output visual features can be directly used for multi-modal prediction. Compared to the modular VL systems, LaConvNet can get rid of large backbone networks, and play roles of feature extraction and multi-modal inference at the same time.

To validate our approach, we conduct extensive experiments on four benchmark datasets, *i.e.*, CLEVR [15], CLEVR-Humans [16], RefCOCO [17] and RefCOCO+ [17], of two VL tasks, *i.e.*, Visual Question Answering (VQA) [15, 16] and Referring Expression Comprehension (REC) [17]. The experimental results not only show the superior performance gains of LaConv as a multi-modal module over a set of state-of-the-art (SOTA) methods, *e.g.*, but also confirm three advantages of LaConvNet as an unified multi-modal network:

- Without the large visual backbone, LaConvNet is much more compact than most existing VL systems.
- LaConvNet can be easily generalized to most VL tasks with a few modifications.
- When training from scratch, LaConvNet shows much better learning ability than existing modular methods.

In conclusion, the proposed LaConvNet are compact, efficient and highly generalized, which is a viable alternative for most vision-and-language tasks.

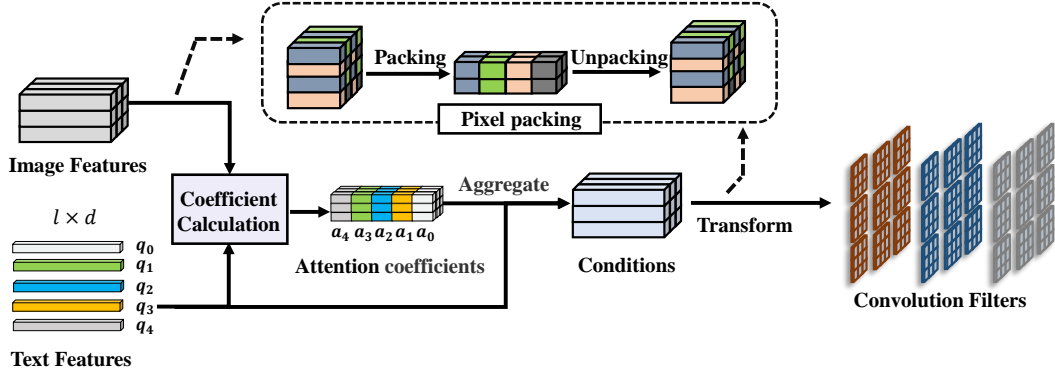


Figure 2: Illustration of the parameter generation based on natural language information. The input text features are first transformed into a language condition matrix by multiplying the affinity matrix between the text and the image features. Then, the convolution filters are predicted based on this condition matrix. A novel *pixel packing* operation is applied to alleviate the *low-rank degeneration* in low-level visual features.

## 2 Language-Guided Dynamic Convolution

In this section, we give the definition of the proposed LaConv, of which structure is illustrated in Fig.1. We begin with the introduction of language-dependent parameter generation, and then describe the dynamic convolution.

### 2.1 Language-conditioned Parameter Generation

As shown in Fig.2, to achieve language-guided visual recognition, LaConv generates dynamic convolution filters based on natural language information. These filters not only depend on the text features, but also on the space and the content of images.

Generally, the length of the text features is often not consistent with the resolution of the image features, and two modalities are also not spatially related. To this end, we first transform the text features into a condition matrix, which has the same shape as the image ones. Each feature vector in this condition matrix is also semantically related to the corresponding image region.

Concretely, given the image features,  $\mathbf{I} \in \mathbb{R}^{(h \times w) \times d}$ , and the text features,  $\mathbf{Q} \in \mathbb{R}^{l \times d}$ , the language condition matrix  $\mathbf{C} \in \mathbb{R}^{(h \times w) \times d}$  is obtained by:

$$\mathbf{C} = \sigma(\mathbf{A}(\mathbf{Q}\mathbf{W}_A)\mathbf{W}_C), \quad (1)$$

Here,  $\sigma$  is the ReLU function, while  $l$  is the length of text,  $h \times w$  denotes the resolution of the image features, and  $d$  is the feature dimension.  $\mathbf{A} \in \mathbb{R}^{(h \times w) \times l}$  is the affinity matrix between  $\mathbf{I}$  and  $\mathbf{Q}$ , and its values denotes the coefficients between the features of two modalities. Here, we resort to *scaled dot-product attention* [43] to compute the multi-modal coefficients:

$$\mathbf{A} = \text{Softmax}\left(\frac{(\mathbf{I}\mathbf{W}_I)^T(\mathbf{Q}\mathbf{W}_Q)}{\sqrt{d}}\right). \quad (2)$$

To improve the module capacity, we also extend Eq. 1 into a *multi-head* version [43].

With Eq.1 and Eq.2, the obtained condition matrix not only has the same shape as the visual features, but also spatially relates to the image regions. Therefore, through the condition matrix, we can effectively embed language information into the dynamic generations of parameters for each visual region and each multi-modal example.

**Pixel packing.** Since the generation of the condition matrix is based on the scale-dot product between two types of features, it can easily lead to the issue of *low-rank degeneration* [3] when the number of the image features is much large than their feature dimension, *e.g.*, low-level image features.

To this end, we propose a novel operation called *pixel packing* to alleviate this problem. As shown in Fig 2, given the image features  $\mathbf{I} \in \mathbb{R}^{(h \times w) \times d}$ , we first pack them into  $k$  new visual tokens, where  $k = (h \times w)/s^2$ , and each token is the concatenation of the  $s \times s$  local features. So, the number of

new image features is reduced by  $s^2$  times. Correspondingly, the resolutions of the condition matrix  $\mathbf{C}$  and the affinity matrix  $\mathbf{A}$  in Eq. 1 also becomes  $(h \times w)/s^2$ . Before the parameter predictions, we will reshape the condition matrix back to the size of  $(h \times w)$ , which is to make sure the predicted filters can adapt the input image features.

Overall, pixel packing can alleviate the issue of low-rank degeneration via reducing the feature resolutions, while maintaining the multi-modal interactions in Eq. 1.

**Convolution filters.** Based on the condition matrix  $\mathbf{C}$ , we further predict the parameters of convolution filters  $\mathbf{W}_{conv} \in \mathbb{R}^{(h \times w) \times (k \times k \times g)}$ , defined as:

$$\mathbf{W}_{conv} = \mathbf{C}\mathbf{W}_1 + b_1. \quad (3)$$

Here,  $k \times k$  denotes the filter size and  $g$  is the number of groups for dynamic convolution.

Although the parameter generation produces a large number of dynamic weights, *i.e.*,  $h \times w \times (k \times k \times g)$  overall, the trainable parameters are only  $k^2gd + 3d^2$ . Compared to a conventional convolution layer, whose parameter size is  $(kd)^2$  and quadratic to the filter size, our parameter generation is still very lightweight.

## 2.2 Language-guided Dynamic Convolution

Based on the generated filters, we further perform dynamic convolutions to achieve language-guided visual feature learning.

This dynamic convolution used in LaConv is principally based on *depth-wise convolution* [22], also known as *group convolution*. Specifically, depth-wise convolution divides the image features into several groups by channel, and its convolutions are independently conducted on each group. The convolution filters are weight-sharing for all spatial regions.

The main differences of LaConv lies in two main aspects. Firstly, each image position  $(i, j)$  has their corresponding filters, which is to model the spatial information in the text features, *e.g.*, “left person”. When filters are shared, such information is hard to recognize. Secondly, based on the predicted filters described in Sec. 2.1., LaConv can extract differentiated visual features of the same image based on different texts. And the output features are highly related to the text.

Concretely, given the grouped image features  $\mathbf{I}^l \in \mathbb{R}^{h \times w \times \frac{d}{g}}$  and the predicted filters  $\mathbf{W} \in \mathbb{R}^{k \times k \times g}$ , the convolution of LaConv is defined as:

$$\begin{aligned} \mathbf{O}_{i,j}^l &= \sum_{\Delta i=1}^k \sum_{\Delta j=1}^k (\mathbf{I}_{R(i,j)}^l)_{\Delta i, \Delta j} \odot \mathbf{W}_{i,j, \Delta i, \Delta j, l}, \\ \mathbf{O} &= \text{concat}(\mathbf{O}^1, \mathbf{O}^2, \dots, \mathbf{O}^g). \end{aligned} \quad (4)$$

Here,  $g$  is the number of groups and  $R(i, j)$  denotes the patch of  $k \times k$  vectors centered on  $\mathbf{I}_{i,j}^l$ ,  $\mathbf{O} \in \mathbb{R}^{h \times w \times d}$  is the output, and  $l$  denotes the index of groups.

Particularly, LaConv does not lead to additional computation compared to the *Depth-wise Convolution*. We also implement LaConv with CUDA kernel, and add it to existing DL libraries, *e.g.*, PyTorch [32], to accelerate the computation.

## 3 LaConvNet

Based on LaConv, we further propose an unified and end-to-end network, termed *LaConvNet*. Its network configurations are given in Tab.1. LaConvNet processes images directly from the pixel level, completely abandoning the traditional convolution backbones like ResNet [9] or MaskRCNN [8]. This property is the main difference of LaConvNet from most existing VL systems, which also makes LaConvNet much more compact.

Besides, we propose three sizes of LaConvNet, namely *LaConvNet-10*, *LaConvNet-15* and *LaConvNet-19*. The suffix indicates the number of LaConv layers. For each stage of LaConvNet, we set a proper *packing size*  $s$  to keep the expressive power of the parameter generation. For the language encoder of LaConvNet, we use 1-layer LSTM unit and 3-layer self-attentions [43].

Output Size	s	LaConvNet-10	LaConvNet-15	LaConvNet-19
$224 \times 224$	-	16-d linear	16-d linear	16-d linear
$112 \times 112$	-	2x2, stride 2 maxpool	2x2, stride 2 maxpool	2x2, stride 2 maxpool
$112 \times 112$	8	3x3, 16-d LaConv $\times$ 2	3x3, 16-d LaConv $\times$ 3	3x3, 16-d LaConv $\times$ 3
$56 \times 56$	-	2x2, stride 2 maxpool	2x2, stride 2 maxpool	2x2, stride 2 maxpool
$56 \times 56$	4	7x7, 64-d LaConv $\times$ 1	7x7, 64-d LaConv $\times$ 2	7x7, 64-d LaConv $\times$ 3
$28 \times 28$	-	2x2, stride 2 maxpool	2x2, stride 2 maxpool	2x2, stride 2 maxpool
$28 \times 28$	2	7x7, 128-d LaConv $\times$ 2	7x7, 128-d LaConv $\times$ 3	7x7, 128-d LaConv $\times$ 4
$14 \times 14$	-	2x2, stride 2 maxpool	2x2, stride 2 maxpool	2x2, stride 2 maxpool
$14 \times 14$	1	7x7, 256-d LaConv $\times$ 4	7x7, 256-d LaConv $\times$ 5	7x7, 256-d LaConv $\times$ 6
$7 \times 7$	-	2x2, stride 2 maxpool	2x2, stride 2 maxpool	2x2, stride 2 maxpool
$7 \times 7$	1	7x7, 512-d LaConv $\times$ 1	7x7, 512-d LaConv $\times$ 2	7x7, 512-d LaConv $\times$ 3
Classifier				

Table 1: Network architecture of LaConvNet. “X-d” denotes the channels of transformations. “s” denotes the packing size of the LaConv block. Similar to ResNet, LaConvNet includes 5 stages and each stage contains several LaConv blocks.

Notably, the design of LaConvNet still has a large space for exploration, such as the choice of depth, width, filter size *etc*. In this paper, we only aim to provide a effective baseline network for the quick validation of our argument. The detailed information of LaConvNet is given in the appendix.

## 4 Experiments

To validate LaConvNet and the LaConv module, we conduct extensive experiments on four benchmark datasets of VQA and REC, namely CLEVR [15], CLEVR-Humans [16], RefCOCO [17] and RefCOCO+ [17], and compare them with a set of SOTA methods [13, 40, 18, 25, 44].

### 4.1 Datasets and Metrics

**CLEVR** [15] is a synthetic VQA dataset introduced by Johnson *et al* [15], which aims to diagnose various reasoning skills, *e.g.*, relations and counting. It contains 999,968 image-question pairs, among which 699,989, 149,991 and 149,998 for training, validation and test, respectively. We use the classification accuracy as the metric.

**CLEVR-Humans** [16] replaces the auto-generated questions in CLEVR with human-annotated ones, which can test the generalization ability of VQA models. It has 17,817, 7,202 and 7,145 examples for training, validation and test, respectively. We use the classification accuracy as the metric.

**RefCOCO & RefCOCO+** [17] are two real-world datasets for referring expression comprehension, which are collected via an interactive game interface. RefCOCO and RefCOCO+ are splitted into *train*, *val*, *test A* and *test B*. The referents of *test A* are about people, while the ones of *test B* are objects. Both datasets have 142,000 expressions for 50,000 bounding boxes of 20,000 images from MS-COCO [23]. The expressions of RefCOCO are mainly about absolute locations, while RefCOCO+ contains more expressions about relative relations and attributes. Following previous works [45, 25], when the Intersection-over-Union (IoU) between prediction and ground-truth is large than 0.5, the prediction is regarded as correct.

### 4.2 Experimental Settings

For CLEVR and CLEVR-Humans, the number of training epochs is 23, and 3 epochs are for warm-up. For RefCOCO and RefCOCO+, the total training epochs are set to 35, 3 of which are for warm-up. We use Glove [33] word embedding with a dimension of 300 to represent each input word. The language encoder is built with an LSTM network and 3 self-attention layers [43], the dimensions of which are 512. The expanding ratio of FFN in LaConv is set to 4. All models are trained by *Adam* optimizer [20]. The basic learning rate is set to 1e-4, which is decayed by a factor of 0.2 at the last third and the last epochs. In default, we use ResNet-34 as the visual backbone for SOTA models

Model	#Params	Overall Accuracy	Count	Cmp. Num.	Exist	Query. Attr.	Cmp. Attr.
BUTD [1]	37M	50.6	44.2	68.7	64.3	44.5	53.7
Film [34]	-	97.6	94.5	93.8	99.2	99.2	99.0
RN [38]	-	95.5	90.1	93.6	97.8	97.1	97.1
BAN [18]	119M	92.2	88.3	94.9	96.4	91.2	94.7
RAMEN [40]	51M	87.8	82.1	83.3	93.9	90.6	87.0
MACNet [13]	27M	98.5	96.7	97.6	99.3	99.3	98.4
LaConvNet-10	14M	98.3	96.4	97.5	99.2	99.3	98.3
LaConvNet-15	20M	98.7	97.4	96.4	99.4	99.5	99.1
LaConvNet-19	26M	<b>99.1</b>	<b>97.9</b>	<b>99.4</b>	<b>99.5</b>	<b>99.6</b>	<b>99.3</b>

Table 2: Comparisons between LaConvNet and SOTAs on CLEVR. All models are trained from scratch. #Params denotes the parameter size<sup>1</sup>.

Model	#Params	RefCOCO			RefCOCO+		
		val	testA	testB	val	testA	testB
MCN-single [25]	24M	56.4	62.3	48.1	39.4	44.7	29.4
One-Stage-BERT [45]	33M	58.5	63.7	51.3	44.9	51.1	36.2
ReSC [44]	31M	58.9	63.8	50.4	44.7	51.3	36.6
LaConvNet-10	12M	60.6	65.1	52.5	49.1	55.1	39.2
LaConvNet-15	18M	60.9	65.2	53.6	49.2	55.3	39.5
LaConvNet-19	24M	<b>62.5</b>	<b>67.9</b>	<b>55.9</b>	<b>49.4</b>	<b>55.7</b>	<b>40.5</b>

Table 3: Comparisons between LaConvNet and SOTAs on RefCOCO and RefCOCO+. All methods are all trained from scratch. #Params denotes the parameters<sup>1</sup>.

to train from scratch. The task-specific head of LaConvNet are borrowed from previous works of VQA [47] and REC [25], respectively. More details can be referred to our supplementary materials.

### 4.3 Experimental Results

#### 4.3.1 Comparison with SOTA Methods

We compare LaConvNet to a set of the SOTA methods [25, 45, 44, 16, 34, 1, 18, 40, 13] on three benchmark datasets, of which results are given in Tab. 2 and Tab. 3. For fair comparisons, all methods are trained on the corresponding dataset from scratch.

CLEVR is a dataset for examining the visual reasoning ability of VL systems, and its scenes and objects are relatively simple. From Tab. 2, we can see that LaConvNets have obvious advantages than SOTA methods in both overall accuracy and parameter size. These results also indicates that LaConvNet not only can extract language-related visual features, but also can achieve efficient multi-modal reasoning. The other observation is that even if the images of CLEVR is very simple, these SOTA modular networks are still affected without backbone pre-training. In contrast, the impact of pre-training on LaConvNet is little, as shown in Tab. 5, suggesting that its unified structure is already capable of learning simple visual knowledge without additional data.

On two real-image datasets, *i.e.*, RefCOCO and RefCOCO+, the advantages of LaConvNets become more prominent. Under the same or fewer parameters, LaConvNet-19 has obvious performance gains over SOTAs ranging from +6.4% to +37.8%. This huge performance gap also reflects the merits of LaConvNet’s unified structure over the modular networks in visual feature learning, especially in RefCOCO+, which focuses on the recognition of low-level information.

But we also noticed that our method still needs an effective pre-training method to further improve the performance of these real-image datasets. This is mainly because real-world images contain many complex scenes and diverse objects, and a limited number of multi-modal samples cannot provide sufficient learning information. The pre-training of LaConvNet will be left in our future work.

<sup>1</sup>The parameters of the language encoder are not included.

(a) Model ablations.			(b) Parameters and computations.		
	LaConvNet-10	Clevr	RefCOCO	Network	Params
+ Base		25.3	30.2	ResNet34 [9]	21.3M
+ Dynamic filters		97.7	57.3	ResNet101 [9]	42.5M
+ Pixel packing		98.3	60.6	LaConvNet-10	10.0M
				LaConvNet-15	15.9M
				LaConvNet-19	21.8M
					3.68G
					7.85G
					1.86G
					2.82G
					3.70G

Table 4: (a). Ablation study of LaConvNet on Clevr *val* set and RefCOCO *val* set. (b). Parameters and computational costs of LaConvNet and two ResNets. MAdds denotes *multiplication-addition* [10], which indicates the computation cost. All results are reported with the image resolution of  $224 \times 224$  and the text length of 15. Parameters and computations of the language encoder are excluded.

Model	Prog.	Overall Accuracy	Humans Before FT	Humans After FT
IEP [16]	700k	96.9	-	-
DDRprog [42]	700k	98.3	-	-
Tbdnet [28]	700k	98.7	-	-
MACNet [13]	0	<u>98.9</u>	<u>57.4</u>	<u>81.5</u>
NS-CL [26]	0	<u>98.9</u>	-	-
LaConv*+ResNet101	0	<b>99.1</b>	<b>58.9</b>	<b>82.4</b>

Table 5: Performance comparison between LaConv and SOTA methods on CLEVR and CLEVR-Humans. *Prog.* denotes the number of extra program ground truths used during training. *LaConv\** is a structure with 6 LaConv layers. The visual backbones of all models are pre-trained on the ImageNet.

#### 4.3.2 Ablation Study

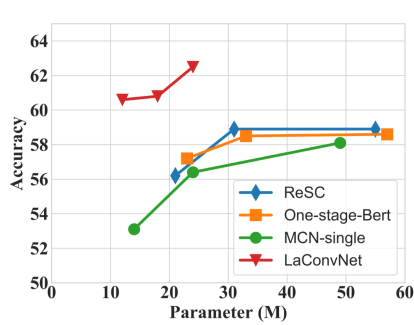
We first examine the effects of dynamic parameter generation and pixel packing of LaConv, of which results are given in Tab. 4 (a). Here, ‘‘Base’’ denotes the single-modal group convolution network, which has a very limited ability to perform multi-modal prediction. As shown in Tab. 4 (a), with the language-dependent parameter generation, the performance of LaConvNet has been greatly improved, indicating its ability to simultaneously process visual information and perform multi-modal reasoning. Another observation is that pixel packing can improve the expressive power of LaConvNet, *e.g.*, +3.3% on RefCOCO, suggesting its effectiveness in dealing with *low-rank degeneration*.

We also validate LaConv as a plug-in module to the existing modular structure, of which results are given in Tab. 5. Specifically, we construct a modular network with 6 LaConv layers and a ResNet101 backbone. From this table we can see that as a multi-modal inference module, LaConv still outperforms SOTA methods with different design principles, such as the symbol-based( TBDNet [28]), Realtion-base (RN [38]) and the attention-based (BAN [18] and BUTD [1]) models. The latest symbol-based method, *i.e.*, Tbdnet [28], uses all program ground-truth during training, which is still inferior than LaConv. Compared to the SOTA method MACNet [13], LaConv is still slightly better, *i.e.*, +0.2%. When transferred to the CLEVR-Humans dataset, the performance gains of LaConv become more obvious, which well confirms its generation ability.

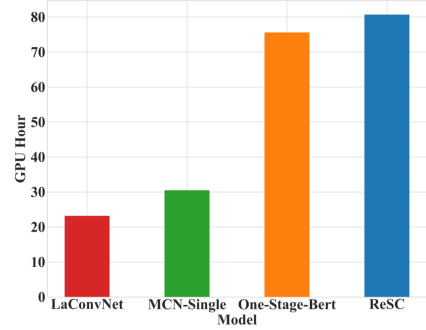
#### 4.3.3 Model Efficiency

The efficiency of LaConvNet are described in Tab.4 (b) and Fig. 3. In Tab.4 (b) , we compare LaConvNet with alternative vision backbones in terms of both parameter size and computation overhead. As a language-conditioned convolution network, LaConvNet is lightweight and efficient. For example, the parameters and computations of LaConvNet-10 are almost 4 times smaller than ResNet101. Considering modular networks require extra modules for language-vision fusions, the compactness of the unified LaConvNet is more distinct. In Fig. 3, we compare LaConvNet with the SOTA modular networks under different parameter sizes<sup>2</sup>. We find that LaConvNet achieves better trade-off between performance and parameters compared to the existing modular models. In term of training efficiency, LaConvNet saves 2/3 training costs against the SOTA REC model, *i.e.*, ReSC [44]. These experiments well support the efficiency of the unified architecture.

<sup>2</sup>We test SOTA model with different backbones, including ResNet18, ResNet34 and ResNet101.



(a) The accuracy-parameter curve.



(b) Training cost of LaConvNet and SOTAs.

Figure 3: (a) Performance comparison between LaConvNet and three SOTA modular networks under different parameter sizes on RefCOCO [17] dataset. (b) Comparisons of training costs between LaConvNet-10 and three SOTA modular networks. The backbone of SOTAs is ResNet101.

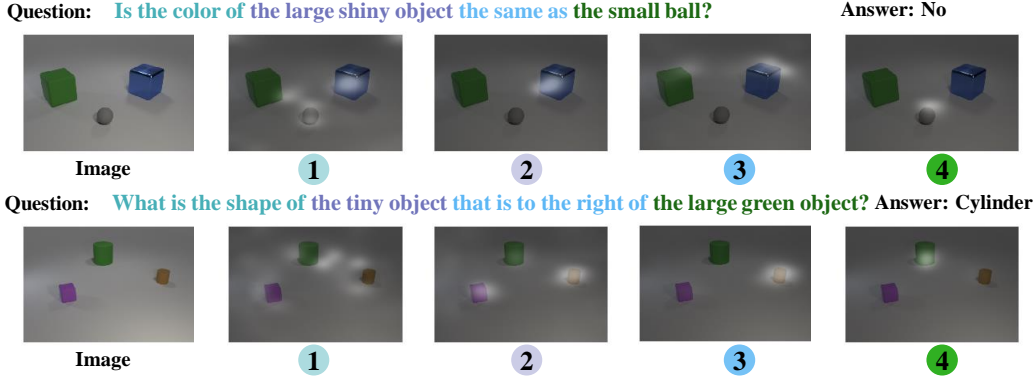


Figure 4: Visualizations of the attention maps in language-conditioned parameter generation. We visualize phrases of a question and their corresponding visual attention. The phrase and the image index of the same colors correspond to each other.

#### 4.3.4 Qualitative Analysis

In this section, we give detailed visualizations to answer two key questions of LaConv and LaConvNet, *i.e.*, “*is the parameter generation reliable and interpretable?*” and “*what convolutions are learned from the natural language instructions?*”

**Is the condition generator reliable and interpretable?** LaConv is more interpretable than the traditional convolution due to the language-dependent parameter generation. To support this argument, we visualize the affinity matrix  $\mathbf{A}$  of its parameter generations. As shown in Fig 4, each phrase of a question attends to the corresponding region. For instance, in the first example of Fig.4, the logical phrase of “the same as” highlights two *same* cubes. Analogically, the spatial phrase of “the right of” in the second example is also related to the *right* object. In addition, other referring phrases, *e.g.*, “the large shiny object” and “the tiny object”, are also visualized in the attention maps. Based on these observations, we believe that the generated convolution filters of a position can accurately execute the corresponding language instructions, which makes LaConv more reliable and interpretable.

**What convolutions are learned from language instructions?** Unlike the conventional convolutions that are weight-sharing for each spatial position, LaConv depends on both image position and text content. To examine its dynamics, we visualize the filters in each stage of LaConvNet in Fig.5. For a better understanding, we select four positions of the example image, and visualize their filters. From Fig.5, the first observation is that the filters for different groups vary greatly (from the vertical axis), which suggests that each group of convolutions is responsible for different recognition patterns. The second observation is that the filters at the initial stage are relatively static, *i.e.*, filters of the same group are similar for different positions (read from the horizontal axis). Such a finding suggests that these

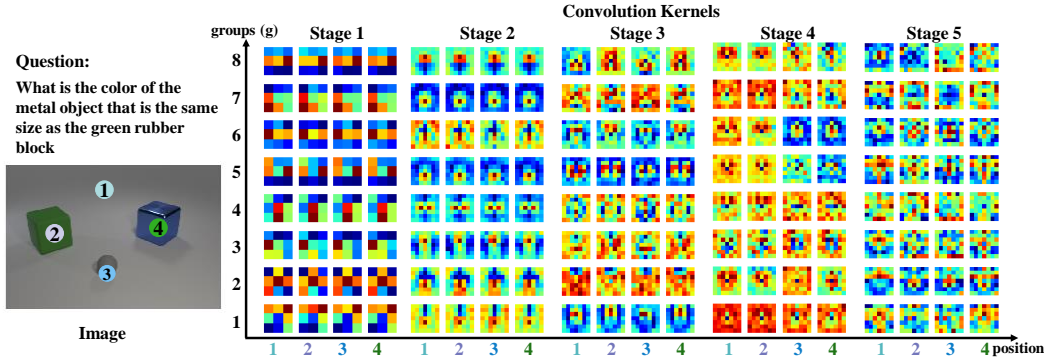


Figure 5: Visualizations of convolution kernels in the LaConvNet-10. Vertical axis denotes each group of convolution kernels. Horizontal axis represents the positions of convolutions that are marked in the image. The colors denote the magnitude of values in filters, and the more red color indicates a larger value. For each stage, we select the last layer for visualization.

convolutions focus on learning low-level visual representations, and they are less affected by natural language information. However, we notice that as the recognition progresses, the filters of the same group vary drastically, presenting different intensities and morphs, *e.g.*, Stage3-5. This observations may suggest that the language instructions start to dynamically guide the visual recognition, therefore different positions present distinct patterns. Conclusively, these visualizations indicates that the language-guided visual recognition of LaConvNet is a continuous process, and the impact of natural language information can be reflected on its weights.

## 5 Related Work

In the latest development of the joint vision-and-language (VL) study, how to equip an VL system with human-like reasoning ability has become the research focus of various VL tasks, such as *visual question answering* [2, 7, 15, 14, 21], *referring expression comprehension* [35, 24, 11, 17, 27]. One of the research direction is to design an inference network that can obtain relevant visual information from the extracted visual features, such as attention-based networks [13, 46], relational network [38] or modulated networks [34, 38]. Differing from these methods, our goal is to use language cues to guide image feature learning in convolutions, thereby integrating the multi-modal reasoning into the visual recognition process. There are several works [34, 31, 5, 6] with similar design principles to ours. Among them, one representative method is FiLM proposed by Perez *et al.* [34], which learns normalization weights by language features and applies them after convolutions. The other is the hybrid convolution proposed by Gao *et al.* [6]. In these methods, the conventional convolution filters are fused by language features and executed in a static convolution, *i.e.*, filters are shared for different images under the same question. In contrast, LaConv generates dynamic language conditions based on both language and visual information, and directly performs language-driven convolutions. The proposed LaConvNet can perform language-guided visual recognition from pixel level, and completely abandon the traditional convolution backbones.

## 6 Conclusion

In this paper, we explore the language-guided visual recognition to achieve a unified reasoning structure for vision-and-language tasks. We first propose a novel language-guided dynamic convolution module called LaConv. With the parameters generated by natural language information, LaConv can complete visual feature learning and multi-modal inference in one forward step. Based on LaConv, we build a fully language-driven network, termed LaConvNet. LaConvNet gets rid of CNN blocks entirely, and directly performs visual reasoning from raw pixels. Extensive experiments are conducted on four benchmarks of two VL tasks, and the experimental results greatly confirm the efficiency and the compactness of the proposed unified network.

## References

- [1] Peter Anderson, Xiaodong He, Chris Buehler, Damien Teney, Mark Johnson, Stephen Gould, and Lei Zhang. Bottom-up and top-down attention for image captioning and visual question answering. In *Proceedings of the IEEE conference on computer vision and pattern recognition*, pages 6077–6086, 2018.
- [2] Stanislaw Antol, Aishwarya Agrawal, Jiasen Lu, Margaret Mitchell, Dhruv Batra, C Lawrence Zitnick, and Devi Parikh. Vqa: Visual question answering. In *Proceedings of the IEEE international conference on computer vision*, pages 2425–2433, 2015.
- [3] Srinadh Bhojanapalli, Chulhee Yun, Ankit Singh Rawat, Sashank Reddi, and Sanjiv Kumar. Low-rank bottleneck in multi-head attention models. In *International Conference on Machine Learning*, pages 864–873. PMLR, 2020.
- [4] Bjoern Bonath, Toemme Noesselt, Antigona Martinez, Jyoti Mishra, Kati Schwiecker, Hans-Jochen Heinze, and Steven A Hillyard. Neural basis of the ventriloquist illusion. *Current Biology*, 17(19):1697–1703, 2007.
- [5] Harm De Vries, Florian Strub, Jérémie Mary, Hugo Larochelle, Olivier Pietquin, and Aaron C Courville. Modulating early visual processing by language. In *Advances in Neural Information Processing Systems*, pages 6594–6604, 2017.
- [6] Peng Gao, Hongsheng Li, Shuang Li, Pan Lu, Yikang Li, Steven CH Hoi, and Xiaogang Wang. Question-guided hybrid convolution for visual question answering. In *Proceedings of the European Conference on Computer Vision (ECCV)*, pages 469–485, 2018.
- [7] Yash Goyal, Tejas Khot, Douglas Summers-Stay, Dhruv Batra, and Devi Parikh. Making the v in vqa matter: Elevating the role of image understanding in visual question answering. In *Proceedings of the IEEE Conference on Computer Vision and Pattern Recognition*, pages 6904–6913, 2017.
- [8] Kaiming He, Georgia Gkioxari, Piotr Dollár, and Ross Girshick. Mask r-cnn. In *Proceedings of the IEEE international conference on computer vision*, pages 2961–2969, 2017.
- [9] Kaiming He, Xiangyu Zhang, Shaoqing Ren, and Jian Sun. Deep residual learning for image recognition. In *Proceedings of the IEEE conference on computer vision and pattern recognition*, pages 770–778, 2016.
- [10] Andrew G Howard, Menglong Zhu, Bo Chen, Dmitry Kalenichenko, Weijun Wang, Tobias Weyand, Marco Andreetto, and Hartwig Adam. Movenets: Efficient convolutional neural networks for mobile vision applications. *arXiv preprint arXiv:1704.04861*, 2017.
- [11] Ronghang Hu, Marcus Rohrbach, Jacob Andreas, Trevor Darrell, and Kate Saenko. Modeling relationships in referential expressions with compositional modular networks. In *CVPR*, 2017.
- [12] Drew Hudson and Christopher D Manning. Learning by abstraction: The neural state machine. In *Advances in Neural Information Processing Systems*, pages 5903–5916, 2019.
- [13] Drew A Hudson and Christopher D Manning. Compositional attention networks for machine reasoning. In *International Conference on Learning Representations*, 2018.
- [14] Drew A Hudson and Christopher D Manning. Gqa: A new dataset for real-world visual reasoning and compositional question answering. In *Proceedings of the IEEE Conference on Computer Vision and Pattern Recognition*, pages 6700–6709, 2019.
- [15] Justin Johnson, Bharath Hariharan, Laurens van der Maaten, Li Fei-Fei, C Lawrence Zitnick, and Ross Girshick. Clevr: A diagnostic dataset for compositional language and elementary visual reasoning. In *Proceedings of the IEEE Conference on Computer Vision and Pattern Recognition*, pages 2901–2910, 2017.
- [16] Justin Johnson, Bharath Hariharan, Laurens Van Der Maaten, Judy Hoffman, Li Fei-Fei, C Lawrence Zitnick, and Ross Girshick. Inferring and executing programs for visual reasoning. In *Proceedings of the IEEE International Conference on Computer Vision*, pages 2989–2998, 2017.
- [17] Sahar Kazemzadeh, Vicente Ordonez, Mark Matten, and Tamara L Berg. Referitgame: Referring to objects in photographs of natural scenes. In *EMNLP*.
- [18] Jin-Hwa Kim, Jaehyun Jun, and Byoung-Tak Zhang. Bilinear attention networks. *arXiv preprint arXiv:1805.07932*, 2018.
- [19] Wonjae Kim, Bokyung Son, and Ildoo Kim. Vilt: Vision-and-language transformer without convolution or region supervision. *arXiv preprint arXiv:2102.03334*, 2021.
- [20] Diederik P Kingma and Jimmy Ba. Adam: A method for stochastic optimization. *arXiv preprint arXiv:1412.6980*, 2014.
- [21] Ranjay Krishna, Yuke Zhu, Oliver Groth, Justin Johnson, Kenji Hata, Joshua Kravitz, Stephanie Chen, Yannis Kalantidis, Li-Jia Li, David A Shamma, et al. Visual genome: Connecting language and vision using crowdsourced dense image annotations. *International journal of computer vision*, 123(1):32–73, 2017.
- [22] Alex Krizhevsky, Ilya Sutskever, and Geoffrey E Hinton. Imagenet classification with deep convolutional neural networks. In *Advances in neural information processing systems*, pages 1097–1105, 2012.
- [23] Tsung-Yi Lin, Michael Maire, Serge Belongie, James Hays, Pietro Perona, Deva Ramanan, Piotr Dollár, and C Lawrence Zitnick. Microsoft coco: Common objects in context. In *European conference on computer vision*, pages 740–755. Springer, 2014.

[24] Runtao Liu, Chenxi Liu, Yutong Bai, and Alan L Yuille. Clevr-ref+: Diagnosing visual reasoning with referring expressions. In *Proceedings of the IEEE Conference on Computer Vision and Pattern Recognition*, pages 4185–4194, 2019.

[25] Gen Luo, Yiyi Zhou, Xiaoshuai Sun, Liujuan Cao, Chenglin Wu, Cheng Deng, and Rongrong Ji. Multi-task collaborative network for joint referring expression comprehension and segmentation. In *Proceedings of the IEEE/CVF Conference on Computer Vision and Pattern Recognition (CVPR)*, June 2020.

[26] Jiayuan Mao, Chuang Gan, Pushmeet Kohli, Joshua B Tenenbaum, and Jiajun Wu. The neuro-symbolic concept learner: Interpreting scenes, words, and sentences from natural supervision. *arXiv preprint arXiv:1904.12584*, 2019.

[27] Junhua Mao, Jonathan Huang, Alexander Toshev, Oana Maria Camбу, Alan L Yuille, and Kevin P Murphy. Generation and comprehension of unambiguous object descriptions. In *CVPR*, 2016.

[28] David Mascharka, Philip Tran, Ryan Soklaski, and Arjun Majumdar. Transparency by design: Closing the gap between performance and interpretability in visual reasoning. In *Proceedings of the IEEE conference on computer vision and pattern recognition*, pages 4942–4950, 2018.

[29] Harry McGurk and John MacDonald. Hearing lips and seeing voices. *Nature*, 264(5588):746–748, 1976.

[30] Louis-Philippe Morency, Rada Mihalcea, and Payal Doshi. Towards multimodal sentiment analysis: Harvesting opinions from the web. In *Proceedings of the 13th international conference on multimodal interfaces*, pages 169–176, 2011.

[31] Duy-Kien Nguyen, Vedanuj Goswami, and Xinlei Chen. Revisiting modulated convolutions for visual counting and beyond. *arXiv preprint arXiv:2004.11883*, 2020.

[32] Adam Paszke, Sam Gross, Francisco Massa, Adam Lerer, James Bradbury, Gregory Chanan, Trevor Killeen, Zeming Lin, Natalia Gimelshein, Luca Antiga, et al. Pytorch: An imperative style, high-performance deep learning library. In *Advances in neural information processing systems*, pages 8026–8037, 2019.

[33] Jeffrey Pennington, Richard Socher, and Christopher D Manning. Glove: Global vectors for word representation. In *Proceedings of the 2014 conference on empirical methods in natural language processing (EMNLP)*, pages 1532–1543, 2014.

[34] Ethan Perez, Florian Strub, Harm de Vries, Vincent Dumoulin, and Aaron C Courville. Film: Visual reasoning with a general conditioning layer. In *AAAI*, 2018.

[35] Bryan A Plummer, Liwei Wang, Chris M Cervantes, Juan C Caicedo, Julia Hockenmaier, and Svetlana Lazebnik. Flickr30k entities: Collecting region-to-phrase correspondences for richer image-to-sentence models. In *Proceedings of the IEEE international conference on computer vision*, pages 2641–2649, 2015.

[36] Soujanya Poria, Erik Cambria, and Alexander Gelbukh. Deep convolutional neural network textual features and multiple kernel learning for utterance-level multimodal sentiment analysis. In *Proceedings of the 2015 conference on empirical methods in natural language processing*, pages 2539–2544, 2015.

[37] Shaoqing Ren, Kaiming He, Ross Girshick, and Jian Sun. Faster r-cnn: Towards real-time object detection with region proposal networks. *arXiv preprint arXiv:1506.01497*, 2015.

[38] Adam Santoro, David Raposo, David G Barrett, Mateusz Malinowski, Razvan Pascanu, Peter Battaglia, and Timothy Lillicrap. A simple neural network module for relational reasoning. In *Advances in neural information processing systems*, pages 4967–4976, 2017.

[39] Ladan Shams, Yukiyasu Kamitani, and Shinsuke Shimojo. Visual illusion induced by sound. *Cognitive brain research*, 14(1):147–152, 2002.

[40] Robik Shrestha, Kushal Kafle, and Christopher Kanan. Answer them all! toward universal visual question answering models. In *Proceedings of the IEEE/CVF Conference on Computer Vision and Pattern Recognition*, pages 10472–10481, 2019.

[41] Barry E Stein and Terrence R Stanford. Multisensory integration: current issues from the perspective of the single neuron. *Nature reviews neuroscience*, 9(4):255–266, 2008.

[42] Joseph Suarez, Justin Johnson, and Fei-Fei Li. Ddrprog: A clevr differentiable dynamic reasoning programmer. *arXiv preprint arXiv:1803.11361*, 2018.

[43] Ashish Vaswani, Noam Shazeer, Niki Parmar, Jakob Uszkoreit, Llion Jones, Aidan N Gomez, Łukasz Kaiser, and Illia Polosukhin. Attention is all you need. In *Advances in neural information processing systems*, pages 5998–6008, 2017.

[44] Zhengyuan Yang, Tianlang Chen, Liwei Wang, and Jiebo Luo. Improving one-stage visual grounding by recursive sub-query construction. *arXiv preprint arXiv:2008.01059*, 2020.

[45] Zhengyuan Yang, Boqing Gong, Liwei Wang, Wenbing Huang, Dong Yu, and Jiebo Luo. A fast and accurate one-stage approach to visual grounding. In *Proceedings of the IEEE/CVF International Conference on Computer Vision*, pages 4683–4693, 2019.

[46] Zichao Yang, Xiaodong He, Jianfeng Gao, Li Deng, and Alex Smola. Stacked attention networks for image question answering. In *Proceedings of the IEEE conference on computer vision and pattern recognition*, pages 21–29, 2016.

[47] Zhou Yu, Jun Yu, Yuhao Cui, Dacheng Tao, and Qi Tian. Deep modular co-attention networks for visual question answering. In *Proceedings of the IEEE/CVF Conference on Computer Vision and Pattern Recognition*, pages 6281–6290, 2019.

- [48] Amir Zadeh, Rowan Zellers, Eli Pincus, and Louis-Philippe Morency. Mosi: multimodal corpus of sentiment intensity and subjectivity analysis in online opinion videos. *arXiv preprint arXiv:1606.06259*, 2016.
- [49] Tianhao Zhang, Hung-Yu Tseng, Lu Jiang, Weilong Yang, Honglak Lee, and Irfan Essa. Text as neural operator: Image manipulation by text instruction. *arXiv preprint arXiv:2008.04556*, 2020.